Analysis of extracellular matrix network dynamics in cancer using the *MatriNet* database

Juho Kontio [a,b,1], Valeria Rolle Soñora [c,1], Vilma Pesola [a], Rijuta Lamba [a,b], Annalena Dittmann [a], Ander Diaz Navarro [d], Jarkko Koivunen [a], Taina Pihlajaniemi [a] and Valerio Izzi [a,b,e]

***a* - Faculty of Biochemistry and Molecular Medicine,** *University of Oulu, Oulu FI-90014, Finland*
***b* - Faculty of Medicine,** *University of Oulu, Oulu FI-90014, Finland*
***c* - Biostatistics and Epidemiology Platform,** *Instituto de Investigación Sanitaria del Principado de Asturias (ISPA), Oviedo, Spain*
***d* - Dpto. de Bioquímica y Biología Molecular,** *IUOPA-Universidad de Oviedo, Oviedo 33006, Spain*
***e* - Foundation for the Finnish Cancer Institute,** *Tukholmankatu 8, Helsinki, Finland*

Corresponding author at: *Faculty of Biochemistry and Molecular Medicine, University of Oulu, Oulu FI-90014, Finland.*
valerio.izzi@oulu.fi.
https://doi.org/10.1016/j.matbio.2022.05.006

Abstract

The extracellular matrix (ECM) is a three-dimensional network of proteins of diverse nature, whose interactions are essential to provide tissues with the correct mechanical and biochemical cues they need for proper development and homeostasis. Changes in the quantity of extracellular matrix (ECM) components and their balance within the tumor microenvironment (TME) accompany and fuel all steps of tumor development, growth and metastasis, and a deeper and more systematic understanding of these processes is fundamental for the development of future therapeutic approaches. The wealth of “big data” from numerous sources has enabled gigantic steps forward in the comprehension of the oncogenic process, also impacting on our understanding of ECM changes in the TME. Most of the available studies, however, have not considered the network nature of ECM and the possibility that changes in the quantity of components might be regulated (co-occur) in cancer and significantly “rebound” on the whole network through its connections, fundamentally altering the matrix interactome. To facilitate the exploration of these network-scale effects we have implemented *MatriNet* (www.matrinet.org), a database enabling the study of structural changes in ECM network architectures as a function of their protein-protein interaction strengths across 20 different tumor types. The use of *MatriNet* is intuitive and offers new insights into tumor-specific as well as pan-cancer features of ECM networks, facilitating the identification of similarities and differences between cancers as well as the visualization of single-tumor events and the prioritization of ECM targets for further experimental investigations.

Introduction

The many hundreds of different proteins assembling into the extracellular matrix (ECM) in tissue specific as well as whole-body assembly patterns regulate the behavior and phenotype of the cells, providing structural and functional cues to tissue architecture and molecular mechanics [1,2].

Quantitative and qualitative alterations to ECM assemblage are a fundamental “footprint” of cancer. The ECM, is, in fact, a major source of chemical and mechanical stimuli influencing intracellular signaling pathways and, as such, is also a crucial controller of the hallmarks of cancers defined by Weinberg and Hanahan [3–5]. Tumors take advantage of manipulating the microenvironment, hence the ECM and all the proteins associated with or impinging on it - collectively known as the matrisome, to condition it to their needs and to the detriment of normal tissues and immunological functions [6]. Almost invariably,

desmoplasia (ECM accumulation) and high collagen content in a neoplastic site are associated with poor patient survival, poor immunological responses, and enhanced cancer growth and spread [6–8]. Whether in physiological or in pathological conditions, changes in ECM quantity or composition impact on the network of interactions that these molecules establish, eventually leading to the formation of *de novo* structures and/or the loss of existing connections [9,10].

Large efforts have been devoted in recent years to the development of algorithms able to reconstruct the structure of biological networks starting from available data [11–13]. The task is not easy nor immediate, as the mathematical constructs and complicacies involved in generating a network that best fits the data provided [14] add to the daunting heterogeneity, time-scale differences and overall quantity of the interactions that characterize biological systems [15].

The enormous importance that ECM connections play in health and disease, and especially in cancer, are a compelling stimulus to develop tools to investigate how the matrix interactome varies in different neoplasms. Beyond the relative "presence" or "absence" of the various proteins, in fact, the study of network patterns informs on systems (or compartments) of ECM interactions being globally active or not, projecting ECM quantities into a space where mechanisms of co-regulation, co-repression or co-evolution can be identified. Recent works defining the landscape of ECM networks [16,17] and the availability of large open data can, in this context, be used to develop a maximum theoretical model listing all the interactions expected to potentially exist, with good confidence, in a system. From this theoretical model we can derive, per each tumor of interest, the connections that are best supported by data and remove the other, obtaining specific ECM network configurations in the same way a sculptor carves a block of marble to "reveal" the final figure.

Following this idea, we have developed *MatriNet* (www.matrinet.org), the first database enabling the investigation of tumor-specific and pan-cancer ECM network modules and differential interaction patterns. These modules, in return, offer both a global view of which proteins are co-present or -absent in one or multiple tumors and also what is the strength of the association between any element of the module, thus identifying different "preferential connections" in otherwise similar interactomes and cancers. In its current implementation (v0.1), *MatriNet* is a proof-of-concept, as it uses a small set of ECM interactions that spans the lysysl oxidase (LOX) and the syndecan (SDs) interactome [18,19]. To calculate the likeliness of the presence or absence of any connection within these interactomes, we used protein profiles from The Human Protein Atlas (THPA) [20]. THPA profiles are a convenient form of data, as they are a direct representation of the quantity of the various ECM proteins they refer to across the different neoplasms. On the other hand, THPA profiles present additional challenges over unidimensional formats (e.g., gene expression or protein abundance values), as they represent *quantitative distributions* of staining across four "levels" (High, Medium, Low and Absent). This means that, to make sense of them, a model needs to "orient" the data in the direction of the levels (High is more than Medium, which is more than Low, which is more than Absent) and calculate the shape of the overall distribution accordingly. Next, the theoretical network model can be updated by comparing the distributions of each pair of interacting proteins and evaluating the association between them. Interactions with high strength will demark areas of the network where proteins co-occur at similar levels in the same samples, while a diminishing strength will denote a loss of co-regulation and, thus, a relative "unlikeliness" of the interaction to occur. Furthermore, using the notion of strength across entire networks, new similarities and specificities can be observed for multiple tumors, offering an unprecedented and systematic view of the ECM interactome.

Results

MatriNet is implemented as a freely-browsable, responsive database available at www.matrinet.org. We have built this resource to enable any matrix biologist to access, analyze and download the structure of ECM networks across cancers through a set of 3 major standalone tools (*MatriNet GX, LX* and *CX*) that can be accessed separately from the *MatriNet* home page.

The leading idea behind *MatriNet* is to superimpose known ECM protein-protein interaction (PPI) networks with quantitative data on each of the node (protein) involved. Each PPI (edge of the network) marks a "possible" or "expected" interaction between two ECM proteins, and the association between the quantities of the two proteins informs on the "likeliness" of such interaction to exist in the network. Intuitively, the higher this value the more likely it is that the two proteins will co-exist and interact in a given tumor's microenvironment, and vice versa. With *MatriNet*, this analysis can be extended to entire networks and, also, used as a starting point to identify (and quantify) similarities and differences among cancers that could not be determined otherwise. A schematic view of how *MatriNet* works is presented in Fig. 1.

The MatriNet homepage. Clicking www.matrinet.org forwards users to the homepage showing our logo and, below, buttons for the 3 tools available for analysis and a project information section. A set of

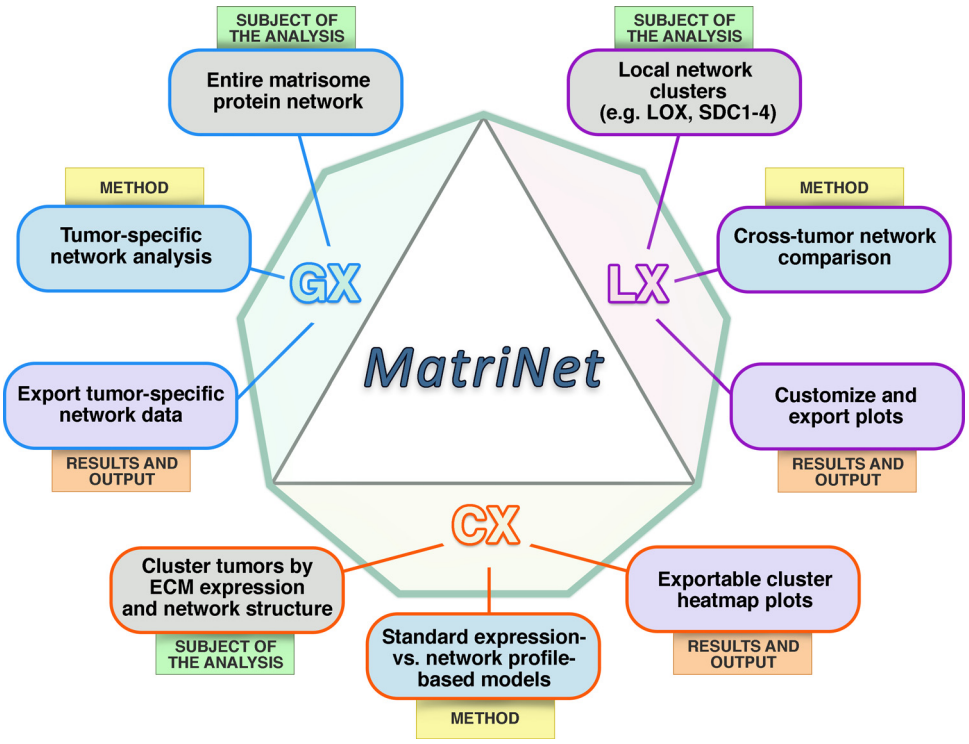

Fig. 1. Schematic view of the *MatriNet* database. The *MatriNet* database is built around 3 tools (GX, LX and CX), which enable the study of single-tumor and pancancer protein-protein association strength across the whole extracellular matrix (ECM) network connectome. The three tools focus on different "levels" of the overall network structure ("subject of the analysis"), employing different algorithms ("methods") to generate tabular and graphical results ("results and outputs") that can be exported from the user.

tutorials for each tool is provided below the application buttons. Each analytical tool is standalone and can be launched independently from the homepage.

The MatriNet GX tool. *MatriNet GX* (where G stands for graph) is the first tool presented by our database and is meant for the exploration of the network structure. The network visualized by default is the "baseline" network sourced from MatrixDB, overlayed with squares of different colors mapping the major subnetworks defined as the neighborhoods of (interactions impinging on) *LOX, SDC1, SDC2, SDC3* and *SDC4*. The network is responsive to user inputs, nodes can be moved freely and the network structure rearranged by means of filtering interactions below or above a user-selected threshold or interval. Also, double-clicking a node selects its neighborhood (all other ECM proteins it is directly linked with) and the rest of the network discarded for easier visualization, and selection of connections can also be obtained by *ctrl*-clicking any given node or *shift*-clicking an area of the network. With the navigation panes on the left and right, parameters pertaining to nodes (proteins) and links (interactions) can be tweaked, filtered, their visibility toggled on and off, etc. Finally, the edge list corresponding to the network being visualized can then be downloaded via the small triangle button at the bottom of the tool and, directly below it, a small information stripe explains the main input and output of the tool, its tweakable parameters and how they affect visualization.

This tool is meant for the visualization of the total network in a specific tumor type, selected via the navigation pane on the left. The landscape of edge weights ("strength" of PPI, equal to the association between any given two proteins) across the network can be explored on a continuous scale with the slider on the left, and all edges outside of the selected range are disconnected from the network. The purpose of this tool is not to suggest a most-trustworthy or -stable network structure as a function of a given edge strength value. Rather, this tool enables at a glance the visualization of nodes whose *connectivity* remains stable or varies at different levels of strength and which connect the most proteins within and across neighborhoods. Also, this tool enables the download of calculated edge strengths and node features (such as the degree) of the nodes and edges selected, providing an immediate access to the actual data the user is looking at.

Usage example: user selects breast cancer and investigates how connections change at different levels of edge strength, for example an interval $0.75-1.00$. Using this specific range of weights, the

user will notice that (1) LOX-cluster is now disconnected completely, the majority of the communications between SDC1 and the other main network cluster have been disaggregated, except for the connection between SDC3. The similar type of pattern can be found by repeating the analysis for the endometrial cancer. Surprisingly, despite its similarity in tissue of origin with the ovarian cancer, the connection between SDC1 and LOX is formed between COL1A1 and COL1A2 proteins, the former of which is also connecting SDC1 and LOX in the cervical cancer. Therefore, it might These neighborhoods and their connections can be further evaluated in the *LX* tool accompanied with external databases such as CBioPortal (https://www.cbioportal.org/) to further investigate their practical relevance. .

A ***tutorial*** portraying the use of *MatriNet GX* can be further found in the *MatriNet* homepage, and a more exhaustive introduction to the use of MatriNet (with examples) is available at https://pdfhost.io/v/cF8.WZdAE_Introduction_to_MatriNet_v01.

The MatriNet LX tool. *MatriNet LX* (where L stands for local structures) is the second tool in the workflow and is tailored to the identification of "network modules" across any of the 20 tumor types available. This tool generates two graphs at the same time, allowing to focus on two aspects of the same query or to compare two different queries. Briefly, the first graph automatically selects all the proteins directly connected to any of the "subnetwork centers" (chosen via the menu on the right) - that is, the neighborhood of the query - and returns the association between the chosen center and all the proteins connected with it. The higher the value the more likely a protein is part of the selected subnetwork (and, as such, could be back-found in the total ECM network by *MatriNet GX*), and vice versa. The second graph considers shortest paths - that is, it identifies all proteins *other than the neighborhood* which are indirectly connected with the chosen center via intermediate nodes (the neighborhood of the center, the neighborhood of the neighborhood, etc.). Given the level of interconnection of the background model, the choice of the shortest path (the shortest "walk" from the subnetwork center to a far away node) gives smaller values to those distant nodes which are "most influenced" from the chosen center, while feeble - though possible - distant network interactions/effects are given a maximum distance value of 1. Hence, in the first graph, the strength of connections *within* a subnetwork is reported, while in the second graph *the influence of a node across* the whole network is reported. The comparison of strength values across cancers in the first graph highlights which ECM proteins are likely connected to a center and which aren't, evidencing the *local* differences in the structure of tumor ECM networks. Conversely, the second graph allows the evaluation and the identification of strong and weak associations across the entire network, whose effects might be important in shaping the total connectivity of the tumor matrisome network.

Usage example: user selects glioma, breast, cervical, endometrial and ovarian cancers from the left menu and then chooses *SDC1* as the center from the drop-down menu on the right. The graph will display five curves of different colors (user can further smooth them via the selector on the right) which largely overlap but for within two areas on the left and right sides of the middle of the graph, curves are separating from each other as both glioma and breast cancer curves dip down significantly. Zooming into this area, the user will find GMEBS1-2 proteins connecting SDC1 with the SDC2 and FYN connecting SDC1 and SDC3 (the left dipping point). Moreover, all other syndecans (SDC2-4) are located right below the other differentiating region on the right. On the other hand, the LOX centered cluster is completely disconnected from the rest of network in the breast cancer and only loosely connected through COL1A1 and COL1A2 within endometrial, cervical and ovarian cancers. In the Glioma network, however, LOX is tightly interacting with SDC1 cluster, not only via COL1A1-2, but also through MMP2 and PLG proteins. We discuss this further in the Discussion section.

Moving to the second graph, and again selecting SDC1 as the center, cervical, endometrial and ovarian cancers appear aligned one after another halfway through the y-axis. A bright azure/white area (indicating stronger "distant effects" of this center) is found towards the end of the x-axis and, by zooming, the user will appreciate the higher influence of SDC1 on, e.g., plasminogen (PLG) in endometrial cancers than in the other. Noticing that PLG connects SDC1 to LOX and recalling from above that other important connection between these two centers, such as MMP2, are likely lost in breast cancers, it can be suggested that SDC1 accounts for the most of the interactions with PLG in this tumor while the same protein is "shared" between different areas of the ECM interactome in other neoplasms.

A tutorial portraying the use of MatriNet LX can be further found in the MatriNet homepage, and a more exhaustive introduction to the use of MatriNet (with examples) is available at https://pdfhost.io/v/cF8.WZdAE_Introduction_to_MatriNet_v01.

The MatriNet CX tool. *MatriNet CX* is the third and last tool in the workflow, built to cluster tumor types using network− and non-network−based approaches (Fig. 1D). A non-network−based approach only uses protein expression profiles, with no regard as to whether the proteins being analyzed interact or not and, thus, likely co-occur or not. Clustering tumors this way can, at best, identify similarities based on global expression pattern profiles. On the other hand, network−based approaches also consider the eventual connections (PPI) between

the proteins being evaluated and groups more closely tumors with similar *local* structures within the ECM network.

This tool is meant to evaluate the amount of similarity and differences among tumors given the underlying data distributions (expression profiles) and/or the network structure encompassing the data. The expression profile-based clustering is what, generally, a user would get from the THPA data with no consideration to the known interactions among these proteins. The network−based approaches, conversely, give high importance to the connections within the network, hence to the co-occurrence of expected interacting pairs and/or the connections between subnetworks. In this respect, the tool provides two alternatives that can be chosen via the selector on the right: a "network edge-weight model", which considers only directly interacting pairs, and a "network flow model" that, much like the second graph in *MatriNet* LX, also considers how strongly each subnetwork connects to any other reachable one as the direct estimation of the association between any two nodes that can be connected by the *shortest walk over* the network. Immediately below, a heatmap reporting the absolute difference in the strength of connection of any ECM protein with its center across all cancers is shown, to ease glancing at the most different subnetwork structures which are likely to have a major impact in driving the network-based clustering algorithms and, potentially, hold a particular biological significance.

Usage example: user selects "Expression-profile model" from the selector on the left and notices that cervical, endometrial and ovarian cancers are separated from each other, clustering in what seems a random order with other carcinomas and generating a heatmap whose most common value is zero (hence, no similarity across tumors). This is the model that would be obtained from the protein expression profiles per se, without consideration to local or distant network structures. Subsequently, the user selects "Network edge-weight model" (a model that gives more importance to neighborhood connectivity) and "Network flow model" (a model that gives more importance to total - neighborhood and distant - connectivity) and notice that meaningful clusters appear, with endometrial, cervical and ovarian tumors never being too far apart.

Scrolling down to the differential networks tool, the user selects cervical and endometrial cancers from the drop-down menu on the left and notices an azure/blue square - indicative of large differences between the two tumors - in the upper left corner of the heatmap, corresponding to the SDC1 neighborhood. Again, zooming, the same genes already identified before appear, with the largest difference mapping to PLG, as discussed before.

A tutorial portraying the use of MatriNet CX can be further found in the MatriNet homepage, and a more exhaustive introduction to the use of MatriNet (with examples) is available at https://pdfhost.io/v/cF8.WZdAE_Introduction_to_MatriNet_v01.

Discussion

Since Paget's pioneering idea of "bad seed in a bad soil" to explain tumorigenesis [21], ECM has been recognized as a fundamental player in all the steps of the oncogenic process and much efforts have been devoted to the identification of ECM components within the TME and their functional relevance [6,22]. A particular aspect of interest, poorly studied, remains however the system-level organization of the tumor ECM, both at the quantitative and qualitative level. In this regard, *MatriNet* is a first attempt at visualizing and analyzing how ECM networks vary across cancers as a function of protein quantity.

Starting from THPA protein staining profiles [20] and MatrixDB network structures [17], *MatriNet* uses an estimator based on the Kullback-Leibler divergence [23] to evaluate association between ECM proteins (the co-occurrence of two proteins) in any of the 20 tumor types for which data are available in THPA. These data are then presented to researchers, allowing for: (1) the visualization of PPI strengths in a tumor, showing which parts of the ECM network are most strongly connected and which are not; (2) the comparison of local network structures (subnetworks) across cancers, enabling the immediate spotting of proteins which are likely present in a given tumor type's subnetwork but missing in another tumor type, and (3) the evaluation of similarities between tumors that are driven by network structures rather than data *per se*.

Using *MatriNet*, local and global patterns of ECM networks can be easily identified and used as a starting point for further analyzes. For example, a researcher could use our database to evaluate similarities and differences among tumors with overlapping cell- and tissue-of-origin patterns [24], such as endometrial and cervical cancer or prostate and testis cancer. In both cases, *MatriNet CX* network-based tools are the only able to appropriately cluster these tumors according to their tissue/system-of-origin, while the model built solely on ECM protein quantity fails poorly. From this starting point, the researcher could use *MatriNet LX* to visualize similarities and differences across the network centers, discovering that, e.g., the *LOX*- and *SDC1*-subnetwork profiles of endometrial and cervical cancers are largely different while the *SDC2-, SDC3-* and *SDC4*-subnetwork are essentially similar. Hence, focusing on the differences within the *LOX* subnetwork, the researcher could immediately notice the

much stronger association of *COL1A2* with LOX in endometrial cancers than in cervical ones, in line with recent observations in patients, *in vitro* and *in silico* [25–27]. Similarly, researchers could appreciate the large difference in the association of *ADAM17* with the subnetwork center (*SDC4*) in the two tumors, a difference that reflects findings on the role of this molecule in cervical cancers [28]. Further, more systematic observations can be made by looking at the absolute difference plot in *MatriNet CX*, facilitating the exploration of fine details within the subnetworks and the generation of novel hypotheses.

MatriNet is in its initial development stage and will be expanded with future releases to accommodate more data and interactions. We strongly encourage user feedback and hope the ECM community will volunteer to provide further data and ideas to implement new functions. A fundamental limitation of *MatriNet* in its current version (v0.1) is the size of the underlying network, covering only a part of the total ECM interactome available from MatrixDB, and the use of only one source (THPA) and one type (antibody staining profiles) of data to evaluate the co-occurrence of ECM proteins. We are currently working on scaling up *MatriNet* to all interactions provided by MatrixDB as well as on the integration of gene expression and clinical data from The Cancer Genome Atlas (TCGA) [29,30] and continuous protein abundance values from the MatrisomeDB [31], to more accurately and more widely analyze ECM network dynamics (eventually, at the proteogenomics level) across cancers. With the scaling up of the database, we will also implement a looser policy in centering the network, allowing users to freely choose any protein as a "subnetwork" center. Another tool currently in development will allow for the comparison of networks between tumors and the corresponding healthy tissues, to provide a differential view [14,32] that could help in further prioritizing local ECM network structures with high specificity to a given tumor. Furthermore, we foresee the implementation of longitudinal studies and spatial information in future releases of *MatriNet* which is still in its initial development stage and very open to contributions from the ECM community.

In conclusion, we believe that the *MatriNet* database offers a new perspective on tumor ECM networks which complements existing databases [17,31] and supports a data-intensive approach to the identification of ECM interaction patterns in cancer.

Experimental procedures

Data. Staining intensity profiles based on immunohistochemistry using tissue micro arrays for the human proteome are sourced from the latest version of The Human Protein Atlas (THPA, http://www.proteinatlas.org) version 21.0, Ensembl version 103.38 at the moment of writing [20]. ECM networks are created from the interactions (edges of the network) present in the MatrixDB database (http://matrixdb.univ-lyon1.fr) [17]. In the current release of MatriNet, the following MatrixDB interaction networks have been used: "Interaction network of the propeptide of lysyl oxidase" - Interactome of LOX Propeptide [19] and "Interaction network of the four syndecans" - Interactome of Syndecans [18], though we plan on expanding the network to all connections available in MatrixDB in future releases.

Database implementation. MatriNet is hosted by shinyapps.io (http:/www.shinyapps.io/). The program is written as a mixture of R, Python, C++, and JavaScript programming languages to ensure a stable and adaptive maintenance environment for controlling version and module updates, as well as scalability. Some of the results are pre-calculated with Python and C++.

Edge weight calculation with entropy estimates. The standard data format for typical network model estimation is to have *P* columns, each of which refers to an individual protein, as well as *N* rows consisting of sample-specific expression values for each protein [33]. Staining profiles from THPA are compositional, i.e., they only represent quantitative distributions of staining across four "levels" (High, Medium, Low and Absent), and thus unusable for the purpose of covariance analysis and classical maximum likelihood-based approaches [34].

To circumvent this limitation, we resorted to information geometry [35] and developed an association measure based on the Kullback-Leibler (KL) divergence [23] between two frequency distributions. In simple terms, KL divergence evaluates the amount of information *lost* if the expression profile of one protein is used to approximate the expression profile of another protein. This implies that the KL divergence measure for completely identical distributions is equal to zero and increases with more diverging expression profiles [35]. The original version of KL divergence is, however, inapplicable to the estimation of network models because of its asymmetry in respect to the order of input distributions (the KL divergence between protein A and protein B, $KLD_{pA \rightarrow pB}$, is not the same as its reciprocal, $KLD_{pB \rightarrow pA}$). In *MatriNet*, we implemented a recursive approach to overcome this limitation. First, each individual edge weight in the network was defined as the average of KLDs calculated separately for both directions ($KLD_{pA \rightarrow pB}$ and $KLD_{pB \rightarrow pA}$), to get the information radius between two expression profile distributions (also known as the Jensen-Shannon, JS, divergence), the outcome of which is demonstrably a symmetric, bounded ([0, 1]) modification of the KL divergence [36,37]. Next, a

new estimator was developed as the inverted interpretation of JS divergence (1 - JS divergence). While the JS divergence converges towards zero as the similarity of input distributions increases (by the definition of KLD), the new estimator converges towards one as the similarity of input distributions increases, matching the standard definition of edge weights in weighted networks as based on similarity measures (i.e., larger edge weight values are associated with stronger associations between nodes). Finally, the new estimator was applied to the calculation of all tumor-specific network edge weights from the protein expression profiles, enabling the interpretation of each edge weight as an analogous to the absolute value of a standard correlation coefficient.

The edge weight clustering model in the *MatriNet* CX model is simply based on computing the Frobenius norm (FN) over the differences of weighted adjacency matrices between tumors [38]. The values appearing in the heatmap are then calculated as 1 - FN to imply that tumor pairs with the smallest amount of network differences (higher similarity) have the largest values [39]. The same measure is used for network flow clustering model, but the original weighted adjacency matrices are replaced with matrices representing shortest weighted distances (sum of weights) between any given pair of proteins [40].

The complete array of analytical procedures employed in *MatriNet* is available in the dedicated GitHub page (see *Data availability*)

Data availability

All pre-processing and analytical procedures are open access and available at https://github.com/lzzi-lab/matrinet.

Acknowledgments

Authors would like to thank Monica Bassignana (www.monicabassignana.com) for designing the MatriNet logo and helping with Fig. 1. This research is connected to the DigiHealth-project, a strategic profiling project at the University of Oulu. The project is supported by the Academy of Finland (project number 326291), the University of Oulu, and the Finnish Cancer Institute, K. Albin Johansson Cancer Research Fellowship fund.

Received 30 January 2022;
Received in revised form 23 April 2022;
Accepted 10 May 2022
Available online 12 May 2022[1]These authors contributed equally to this work.

References

[1] I.N. Taha, A. Naba, Exploring the extracellular matrix in health and disease using proteomics, Essays Biochem. 63 (2019) 417–432, doi: 10.1042/EBC20190001.
[2] A.D. Theocharis, S.S. Skandalis, C. Gialeli, N.K. Karamanos, Extracellular matrix structure, Adv. Drug. Deliv. Rev. 97 (2016) 4–27, doi: 10.1016/j.addr.2015.11.001.
[3] D. Hanahan, R.A. Weinberg, Hallmarks of cancer: the next generation, Cell 144 (2011) 646–674, doi: 10.1016/j.cell.2011.02.013.
[4] M.W. Pickup, J.K. Mouw, V.M. Weaver, The extracellular matrix modulates the hallmarks of cancer, EMBO Rep. 15 (2014) 1243–1253, doi: 10.15252/embr.201439246.
[5] A.E. Yuzhalin, S.Y. Lim, A.G. Kutikhin, A.N. Gordon-Weeks, Dynamic matrisome: ECM remodeling factors licensing cancer progression and metastasis, Biochim. Biophys. Acta Rev. Cancer 1870 (2018) 207–228, doi: 10.1016/j.bbcan.2018.09.002.
[6] A.M. Socovich, A. Naba, The cancer matrisome: from comprehensive characterization to biomarker discovery, Semin. Cell Dev. Biol. 89 (2019) 157–166, doi: 10.1016/j.semcdb.2018.06.005.
[7] C. Tian, D. Öhlund, S. Rickelt, T. Lidström, Y. Huang, L. Hao, R.T. Zhao, O. Franklin, S.N. Bhatia, D.A. Tuveson, R.O. Hynes, Cancer-cell-derived matrisome proteins promote metastasis in pancreatic ductal adenocarcinoma, Cancer Res. (2020), doi: 10.1158/0008-5472.CAN-19-2578.
[8] V. Izzi, J. Lakkala, R. Devarajan, A. Kääriäinen, J. Koivunen, R. Heljasvaara, T. Pihlajaniemi, Pan-cancer analysis of the expression and regulation of matrisome genes across 32 tumor types, Matrix Biol. Plus 1 (2019) 100004, doi: 10.1016/j.mbplus.2019.04.001.
[9] M. Paolillo, S. Schinelli, Extracellular matrix alterations in metastatic processes, Int. J. Mol. Sci. 20 (2019) E4947, doi: 10.3390/ijms20194947.
[10] J. Winkler, A. Abisoye-Ogunniyan, K.J. Metcalf, Z. Werb, Concepts of extracellular matrix remodelling in tumour progression and metastasis, Nat. Commun. 11 (2020) 5120, doi: 10.1038/s41467-020-18794-x.
[11] C. Liu, Y. Ma, J. Zhao, R. Nussinov, Y.C. Zhang, F. Cheng, Z.K. Zhang, Computational network biology: data, models, and applications, Phys. Rep. 846 (2020) 1–66, doi: 10.1016/j.physrep.2019.12.004.
[12] M. Ghanbari, J. Lasserre, M. Vingron, Reconstruction of gene networks using prior knowledge, BMC Syst. Biol. 9 (2015) 84, doi: 10.1186/s12918-015-0233-4.
[13] M. Koutrouli, E. Karatzas, D. Paez-Espino, G.A. Pavlopoulos, A guide to conquer the biological network era using graph theory, Front. Bioeng. Biotechnol. 8 (2020) 34, doi: 10.3389/fbioe.2020.00034.
[14] J.A.J. Kontio, M.J. Rinta-Aho, M.J. Sillanpää, Estimating linear and nonlinear gene coexpression networks by semiparametric neighborhood selection, Genetics 215 (2020) 597–607, doi: 10.1534/genetics.120.303186.
[15] J. Cha, I. Lee, Single-cell network biology for resolving cellular heterogeneity in human diseases, Exp. Mol. Med. 52 (2020) 1798–1808, doi: 10.1038/s12276-020-00528-0.
[16] S. Ricard-Blum, A. Naba, The extracellular matrix goes -Omics: resources and tools, in: Extracellular Matrix Omics, Springer, Accepted.
[17] O. Clerc, M. Deniaud, S.D. Vallet, A. Naba, A. Rivet, S. Perez, N. Thierry-Mieg, S. Ricard-Blum, MatrixDB:

integration of new data with a focus on glycosaminoglycan interactions, Nucleic Acids Res. 47 (2019) D376–D381, doi: 10.1093/nar/gky1035.

[18] F. Gondelaud, S. Ricard-Blum, Structures and interactions of syndecans, FEBS J. 286 (2019) 2994–3007, doi: 10.1111/febs.14828.

[19] S.D. Vallet, A.E. Miele, U. Uciechowska-Kaczmarzyk, A. Liwo, B. Duclos, S.A. Samsonov, S. Ricard-Blum, Insights into the structure and dynamics of lysyl oxidase propeptide, a flexible protein with numerous partners, Sci. Rep. 8 (2018) 11768, doi: 10.1038/s41598-018-30190-6.

[20] M. Uhlén, L. Fagerberg, B.M. Hallström, C. Lindskog, P. Oksvold, A. Mardinoglu, Å. Sivertsson, C. Kampf, E. Sjöstedt, A. Asplund, I. Olsson, K. Edlund, E. Lundberg, S. Navani, C.A.K. Szigyarto, J. Odeberg, D. Djureinovic, J.O. Takanen, S. Hober, T. Alm, P.H. Edqvist, H. Berling, H. Tegel, J. Mulder, J. Rockberg, P. Nilsson, J.M. Schwenk, M. Hamsten, K. von Feilitzen, M. Forsberg, L. Persson, F. Johansson, M. Zwahlen, G. von Heijne, J. Nielsen, F. Pontén, Proteomics. Tissue-based map of the human proteome, Science 347 (2015) 1260419, doi: 10.1126/science.1260419.

[21] R.R. Langley, I.J. Fidler, The seed and soil hypothesis revisited - the role of tumor-stroma interactions in metastasis to different organs, Int. J. Cancer 128 (2011) 2527–2535, doi: 10.1002/ijc.26031.

[22] E.C. Filipe, J.L. Chitty, T.R. Cox, Charting the unexplored extracellular matrix in cancer, Int. J. Exp. Pathol. 99 (2018) 58–76, doi: 10.1111/iep.12269.

[23] S. Kullback, R.A. Leibler, On information and sufficiency, Ann. Math. Stat. 22 (1951) 79–86, doi: 10.1214/aoms/1177729694.

[24] K.A. Hoadley, C. Yau, T. Hinoue, D.M. Wolf, A.J. Lazar, E. Drill, R. Shen, A.M. Taylor, A.D. Cherniack, V. Thorsson, R. Akbani, R. Bowlby, C.K. Wong, M. Wiznerowicz, F. Sanchez-Vega, A.G. Robertson, B.G. Schneider, M.S. Lawrence, H. Noushmehr, T.M. Malta, S.J. Caesar-Johnson, J.A. Demchok, I. Felau, M. Kasapi, M.L. Ferguson, C.M. Hutter, H.J. Sofia, R. Tarnuzzer, Z. Wang, L. Yang, J.C. Zenklusen, J. (Julia) Zhang, S. Chudamani, J. Liu, L. Lolla, R. Naresh, T. Pihl, Q. Sun, Y. Wan, Y. Wu, J. Cho, T. DeFreitas, S. Frazer, N. Gehlenborg, G. Getz, D.I. Heiman, J. Kim, M.S. Lawrence, P. Lin, S. Meier, M.S. Noble, G. Saksena, D. Voet, H. Zhang, B. Bernard, N. Chambwe, V. Dhankani, T. Knijnenburg, R. Kramer, K. Leinonen, Y. Liu, M. Miller, S. Reynolds, I. Shmulevich, V. Thorsson, W. Zhang, R. Akbani, B.M. Broom, A.M. Hegde, Z. Ju, R.S. Kanchi, A. Korkut, J. Li, H. Liang, S. Ling, W. Liu, Y. Lu, G.B. Mills, K.S. Ng, A. Rao, M. Ryan, J. Wang, J.N. Weinstein, J. Zhang, A. Abeshouse, J. Armenia, D. Chakravarty, W.K. Chatila, I. de Bruijn, J. Gao, B.E. Gross, Z.J. Heins, R. Kundra, K. La, M. Ladanyi, A. Luna, M.G. Nissan, A. Ochoa, S.M. Phillips, E. Reznik, F. Sanchez-Vega, C. Sander, N. Schultz, R. Sheridan, S.O. Sumer, Y. Sun, B.S. Taylor, J. Wang, H. Zhang, P. Anur, M. Peto, P. Spellman, C. Benz, J.M. Stuart, C.K. Wong, C. Yau, D.N. Hayes, J.S. Parker, M.D. Wilkerson, A. Ally, M. Balasundaram, R. Bowlby, D. Brooks, R. Carlsen, E. Chuah, N. Dhalla, R. Holt, S.J.M. Jones, K. Kasaian, D. Lee, Y. Ma, M.A. Marra, M. Mayo, R.A. Moore, A.J. Mungall, K. Mungall, A.G. Robertson, S. Sadeghi, J.E. Schein, P. Sipahimalani, A. Tam, N. Thiessen, K. Tse, T. Wong, A.C. Berger, R. Beroukhim, A.D. Cherniack, C. Cibulskis, S.B. Gabriel, G.F. Gao, G. Ha, M. Meyerson, S.E. Schumacher, J. Shih, M.H. Kucherlapati, R.S. Kucherlapati, S. Baylin, L. Cope, L. Danilova, M.S. Bootwalla, P.H. Lai, D.T. Maglinte, D.J.V.D. Berg, D.J. Weisenberger, J.T. Auman, S. Balu, T. Bodenheimer, C. Fan, K.A. Hoadley, A.P. Hoyle, S.R. Jefferys, C.D. Jones, S. Meng, P.A. Mieczkowski, L.E. Mose, A.H. Perou, C.M. Perou, J. Roach, Y. Shi, J.V. Simons, T. Skelly, M.G. Soloway, D. Tan, U. Veluvolu, H. Fan, T. Hinoue, P.W. Laird, H. Shen, W. Zhou, M. Bellair, K. Chang, K. Covington, C.J. Creighton, H. Dinh, H. Doddapaneni, L.A. Donehower, J. Drummond, R.A. Gibbs, R. Glenn, W. Hale, Y. Han, J. Hu, V. Korchina, S. Lee, L. Lewis, W. Li, X. Liu, M. Morgan, D. Morton, D. Muzny, J. Santibanez, M. Sheth, E. Shinbrot, L. Wang, M. Wang, D.A. Wheeler, L. Xi, F. Zhao, J. Hess, E.L. Appelbaum, M. Bailey, M.G. Cordes, L. Ding, C.C. Fronick, L.A. Fulton, R.S. Fulton, C. Kandoth, E.R. Mardis, M.D. McLellan, C.A. Miller, H.K. Schmidt, R.K. Wilson, D. Crain, E. Curley, J. Gardner, K. Lau, D. Mallery, S. Morris, J. Paulauskis, R. Penny, C. Shelton, T. Shelton, M. Sherman, E. Thompson, P. Yena, J. Bowen, J.M. Gastier-Foster, M. Gerken, K.M. Leraas, T.M. Lichtenberg, N.C. Ramirez, L. Wise, E. Zmuda, N. Corcoran, T. Costello, C. Hovens, A.L. Carvalho, A.C. de Carvalho, J.H. Fregnani, A. Longatto-Filho, R.M. Reis, C. Scapulatempo-Neto, H.C.S. Silveira, D.O. Vidal, A. Burnette, J. Eschbacher, B. Hermes, A. Noss, R. Singh, M.L. Anderson, P.D. Castro, M. Ittmann, D. Huntsman, B. Kohl, X. Le, R. Thorp, C. Andry, E.R. Duffy, V. Lyadov, O. Paklina, G. Setdikova, A. Shabunin, M. Tavobilov, C. McPherson, R. Warnick, R. Berkowitz, D. Cramer, C. Feltmate, N. Horowitz, A. Kibel, M. Muto, C.P. Raut, A. Malykh, J.S. Barnholtz-Sloan, W. Barrett, K. Devine, J. Fulop, Q.T. Ostrom, K. Shimmel, Y. Wolinsky, A.E. Sloan, A.D. Rose, F. Giuliante, M. Goodman, B.Y. Karlan, C.H. Hagedorn, J. Eckman, J. Harr, J. Myers, K. Tucker, L.A. Zach, B. Deyarmin, H. Hu, L. Kvecher, C. Larson, R.J. Mural, S. Somiari, A. Vicha, T. Zelinka, J. Bennett, M. Iacocca, B. Rabeno, P. Swanson, M. Latour, L. Lacombe, B. Têtu, A. Bergeron, M. McGraw, S.M. Staugaitis, J. Chabot, H. Hibshoosh, A. Sepulveda, T. Su, T. Wang, O. Potapova, O. Voronina, L. Desjardins, O. Mariani, S. Roman-Roman, X. Sastre, M.H. Stern, F. Cheng, S. Signoretti, A. Berchuck, D. Bigner, E. Lipp, J. Marks, S. McCall, R. McLendon, A. Secord, A. Sharp, M. Behera, D.J. Brat, A. Chen, K. Delman, S. Force, F. Khuri, K. Magliocca, S. Maithel, J.J. Olson, T. Owonikoko, A. Pickens, S. Ramalingam, D.M. Shin, G. Sica, E.G.V. Meir, H. Zhang, W. Eijckenboom, A. Gillis, E. Korpershoek, L. Looijenga, W. Oosterhuis, H. Stoop, K.E. van Kessel, E.C. Zwarthoff, C. Calatozzolo, L. Cuppini, S. Cuzzubbo, F. DiMeco, G. Finocchiaro, L. Mattei, A. Perin, B. Pollo, C. Chen, J. Houck, P. Lohavanichbutr, A. Hartmann, C. Stoehr, R. Stoehr, H. Taubert, S. Wach, B. Wullich, W. Kycler, D. Murawa, M. Wiznerowicz, K. Chung, W.J. Edenfield, J. Martin, E. Baudin, G. Bubley, R. Bueno, A.D. Rienzo, W.G. Richards, S. Kalkanis, T. Mikkelsen, H. Noushmehr, L. Scarpace, N. Girard, M. Aymerich, E. Campo, E. Giné, A.L. Guillermo, N.V. Bang, P.T. Hanh, B.D. Phu, Y. Tang, H. Colman, K. Evason, P.R. Dottino, J.A. Martignetti, H. Gabra, H. Juhl, T. Akeredolu, S. Stepa, D. Hoon, K. Ahn, K.J. Kang, F. Beuschlein, A. Breggia, M. Birrer, D. Bell, M. Borad, A.H. Bryce, E. Castle, V. Chandan, J. Cheville, J.A. Copland, M. Farnell, T. Flotte,

N. Giama, T. Ho, M. Kendrick, J.P. Kocher, K. Kopp, C. Moser, D. Nagorney, D. O'Brien, B.P. O'Neill, T. Patel, G. Petersen, F. Que, M. Rivera, L. Roberts, R. Smallridge, T. Smyrk, M. Stanton, R.H. Thompson, M. Torbenson, J.D. Yang, L. Zhang, F. Brimo, J.A. Ajani, A.M.A. Gonzalez, C. Behrens, O. Bondaruk, R. Broaddus, B. Czerniak, B. Esmaeli, J. Fujimoto, J. Gershenwald, C. Guo, A.J. Lazar, C. Logothetis, F. Meric-Bernstam, C. Moran, L. Ramondetta, D. Rice, A. Sood, P. Tamboli, T. Thompson, P. Troncoso, A. Tsao, I. Wistuba, C. Carter, L. Haydu, P. Hersey, V. Jakrot, H. Kakavand, R. Kefford, K. Lee, G. Long, G. Mann, M. Quinn, R. Saw, R. Scolyer, K. Shannon, A. Spillane, J. Stretch, M. Synott, J. Thompson, J. Wilmott, H. Al-Ahmadie, T.A. Chan, R. Ghossein, A. Gopalan, D.A. Levine, V. Reuter, S. Singer, B. Singh, N.V. Tien, T. Broudy, C. Mirsaidi, P. Nair, P. Drwiega, J. Miller, J. Smith, H. Zaren, J.W. Park, N.P. Hung, E. Kebebew, W.M. Linehan, A.R. Metwalli, K. Pacak, P.A. Pinto, M. Schiffman, L.S. Schmidt, C.D. Vocke, N. Wentzensen, R. Worrell, H. Yang, M. Moncrieff, C. Goparaju, J. Melamed, H. Pass, N. Botnariuc, I. Caraman, M. Cernat, I. Chemencedji, A. Clipca, S. Doruc, G. Gorincioi, S. Mura, M. Pirtac, I. Stancul, D. Tcaciuc, M. Albert, I. Alexopoulou, A. Arnaout, J. Bartlett, J. Engel, S. Gilbert, J. Parfitt, H. Sekhon, G. Thomas, D.M. Rassl, R.C. Rintoul, C. Bifulco, R. Tamakawa, W. Urba, N. Hayward, H. Timmers, A. Antenucci, F. Facciolo, G. Grazi, M. Marino, R. Merola, R. de Krijger, A.P. Gimenez-Roqueplo, A. Piché, S. Chevalier, G. McKercher, K. Birsoy, G. Barnett, C. Brewer, C. Farver, T. Naska, N.A. Pennell, D. Raymond, C. Schilero, K. Smolenski, F. Williams, C. Morrison, J.A. Borgia, M.J. Liptay, M. Pool, C.W. Seder, K. Junker, L. Omberg, M. Dinkin, G. Manikhas, D. Alvaro, M.C. Bragazzi, V. Cardinale, G. Carpino, E. Gaudio, D. Chesla, S. Cottingham, M. Dubina, F. Moiseenko, R. Dhanasekaran, K.F. Becker, K.P. Janssen, J. Slotta-Huspenina, M.H. Abdel-Rahman, D. Aziz, S. Bell, C.M. Cebulla, A. Davis, R. Duell, J.B. Elder, J. Hilty, B. Kumar, J. Lang, N.L. Lehman, R. Mandt, P. Nguyen, R. Pilarski, K. Rai, L. Schoenfield, K. Senecal, P. Wakely, P. Hansen, R. Lechan, J. Powers, A. Tischler, W.E. Grizzle, K.C. Sexton, A. Kastl, J. Henderson, S. Porten, J. Waldmann, M. Fassnacht, S.L. Asa, D. Schadendorf, M. Couce, M. Graefen, H. Huland, G. Sauter, T. Schlomm, R. Simon, P. Tennstedt, O. Olabode, M. Nelson, O. Bathe, P.R. Carroll, J.M. Chan, P. Disaia, P. Glenn, R.K. Kelley, C.N. Landen, J. Phillips, M. Prados, J. Simko, K. Smith-McCune, S. VandenBerg, K. Roggin, A. Fehrenbach, A. Kendler, S. Sifri, R. Steele, A. Jimeno, F. Carey, I. Forgie, M. Mannelli, M. Carney, B. Hernandez, B. Campos, C. Herold-Mende, C. Jungk, A. Unterberg, A. von Deimling, A. Bossler, J. Galbraith, L. Jacobus, M. Knudson, T. Knutson, D. Ma, M. Milhem, R. Sigmund, A.K. Godwin, R. Madan, H.G. Rosenthal, C. Adebamowo, S.N. Adebamowo, A. Boussioutas, D. Beer, T. Giordano, A.M. Mes-Masson, F. Saad, T. Bocklage, L. Landrum, R. Mannel, K. Moore, K. Moxley, R. Postier, J. Walker, R. Zuna, M. Feldman, F. Valdivieso, R. Dhir, J. Luketich, E.M.M. Pinero, M. Quintero-Aguilo, C.G. Carlotti, J.S.D. Santos, R. Kemp, A. Sankarankuty, D. Tirapelli, J. Catto, K. Agnew, E. Swisher, J. Creaney, B. Robinson, C.S. Shelley, E.M. Godwin, S. Kendall, C. Shipman, C. Bradford, T. Carey, A. Haddad, J. Moyer, L. Peterson, M. Prince, L. Rozek, G. Wolf, R. Bowman, K.M. Fong, I. Yang, R. Korst, W.K. Rathmell, J.L. Fantacone-Campbell, J.A. Hooke, A.J. Kovatich, C.D. Shriver, J. DiPersio, B. Drake, R. Govindan, S. Heath, T. Ley, B.V. Tine, P. Westervelt, M.A. Rubin, J.I. Lee, N.D. Aredes, A. Mariamidze, J.M. Stuart, C.C. Benz, P.W. Laird, Cell-of-origin patterns dominate the molecular classification of 10,000 tumors from 33 types of cancer, Cell 173 (2018) 291−304.e6, doi:10.1016/j.cell.2018.03.022.

[25] X. Hu, Y. Bian, X. Wen, M. Wang, Y. Li, X. Wan, Collagen triple helix repeat containing 1 promotes endometrial cancer cell migration by activating the focal adhesion kinase signaling pathway, Exp. Ther. Med. 20 (2020) 1405–1414, doi: 10.3892/etm.2020.8833.

[26] A. Stejskalová, V. Fincke, M. Nowak, Y. Schmidt, K. Borrmann, M.K. von Wahlde, S.D. Schäfer, L. Kiesel, B. Greve, M. Götte, Collagen I triggers directional migration, invasion and matrix remodeling of stroma cells in a 3D spheroid model of endometriosis, Sci. Rep. 11 (2021) 4115, doi: 10.1038/s41598-021-83645-8.

[27] V.K. Yadav, T.Y. Lee, J.B.K. Hsu, H.D. Huang, W.C.V. Yang, T.H. Chang, Computational analysis for identification of the extracellular matrix molecules involved in endometrial cancer progression, PLoS One 15 (2020) e0231594, doi: 10.1371/journal.pone.0231594.

[28] Q. Xu, M. Ying, G. Chen, A. Lin, Y. Xie, N. Ohara, D. Zhou, ADAM17 is associated with EMMPRIN and predicts poor prognosis in patients with uterine cervical carcinoma, Tumour Biol. 35 (2014) 7575–7586, doi: 10.1007/s13277-014-1990-1.

[29] G.F. Gao, J.S. Parker, S.M. Reynolds, T.C. Silva, L.B. Wang, W. Zhou, R. Akbani, M. Bailey, S. Balu, B.P. Berman, D. Brooks, H. Chen, A.D. Cherniack, J.A. Demchok, L. Ding, I. Felau, S. Gaheen, D.S. Gerhard, D.I. Heiman, K.M. Hernandez, K.A. Hoadley, R. Jayasinghe, A. Kemal, T.A. Knijnenburg, P.W. Laird, M.K.A. Mensah, A.J. Mungall, A.G. Robertson, H. Shen, R. Tarnuzzer, Z. Wang, M. Wyczalkowski, L. Yang, J.C. Zenklusen, Z. Zhang, H. Liang, M.S. Noble, Genomic Data Analysis Network,, Before and after: comparison of legacy and harmonized TCGA genomic data commons' data, Cell Syst. 9 (2019) 24–34.e10, doi: 10.1016/j.cels.2019.06.006.

[30] J. Liu, T. Lichtenberg, K.A. Hoadley, L.M. Poisson, A.J. Lazar, A.D. Cherniack, A.J. Kovatich, C.C. Benz, D.A. Levine, A.V. Lee, L. Omberg, D.M. Wolf, C.D. Shriver, V. Thorsson, H. Hu, Cancer Genome Atlas Research Network, An integrated TCGA pan-cancer clinical data resource to drive high-quality survival outcome analytics, Cell 173 (2018) 400–416.e11, doi: 10.1016/j.cell.2018.02.052.

[31] X. Shao, I.N. Taha, K.R. Clauser, Y.T. Gao, A. Naba, MatrisomeDB: the ECM-protein knowledge database, Nucleic Acids Res. 48 (2020) D1136–D1144, doi: 10.1093/nar/gkz849.

[32] J.A.J. Kontio, T. Pyhäjärvi, M.J. Sillanpää, Model guided trait-specific co-expression network estimation as a new perspective for identifying molecular interactions and pathways, PLoS Comput. Biol. 17 (2021) e1008960, doi: 10.1371/journal.pcbi.1008960.

[33] N. Pržulj, Network Medicine, Analyzing Network Data in Biology and Medicine: An Interdisciplinary Textbook for Biological, Medical and Computational Scientists, Cambridge University Press, Cambridge, 2019, pp. 414–458, doi: 10.1017/9781108377706.011.

[34] M. Maathuis, M. Drton, S. Lauritzen, M. Wainwright, Handbook of Graphical Models, CRC Press, Boca Raton, 2018, doi: 10.1201/9780429463976.

[35] F. Nielsen, An elementary introduction to information geometry, Entropy 22 (2020) 1100, doi: 10.3390/e22101100.
[36] J. Lin, Divergence measures based on the Shannon entropy, IEEE Trans. Inf. Theory 37 (1991) 145–151, doi: 10.1109/18.61115.
[37] F. Nielsen, On a generalization of the Jensen−Shannon divergence and the Jensen−Shannon centroid, Entropy 22 (2020) 221, doi: 10.3390/e22020221.
[38] B. Noble, J.W. Daniel, Applied linear algebra, Englewood Cliffs, 2nd ed: Prentice-Hall, London, 1977.
[39] C. Donnat, S. Holmes, Tracking network dynamics: a survey of distances and similarity metrics, ArXiv:1801.07351 [Physics, Stat]. (2018). http://arxiv.org/abs/1801.07351 (accessed January 28, 2022).
[40] D.K. Hammond, Y. Gur, C.R. Johnson, Graph diffusion distance: a difference measure for weighted graphs based on the graph Laplacian exponential kernel, in: Proceedings of the IEEE Global Conference on Signal and Information Processing, 2013, pp. 419–422, doi: 10.1109/GlobalSIP.2013.6736904.